

**Supplemental information for
Behavior of Water in Collagen and
Hydroxyapatite Sites of Cortical Bone:
Fracture, Mechanical Wear, and Load Bearing
Studies**

Farhana Gul-E-Noor,[†] Chandan Singh,^{‡,¶} Antonios Papaioannou,[§] Neeraj
Sinha,[‡] and Gregory S. Boutis^{*,†,§}

*[†]Department of Physics, Brooklyn College of The City University of New York, Brooklyn, New
York 11210, United States*

[‡]Center of Biomedical Research, SGPGIMS Campus, Raibareilly Road, Lucknow 226014, India

[¶]School of Biotechnology, Banaras Hindu University, Varanasi 221005 India

*[§]The Graduate Center of The City University of New York, Department of Physics, New York,
United States*

E-mail: gboutis@brooklyn.cuny.edu

Phone: +1 718951-5000 x2873

The complete author list for Reference 11 and 13 which has more than 10 authors

(11) McElderry, J.-D. P.; Zhu, P.; Mroue, K. H.; Xu, J.; Pavan, B.; Fang, M.; Zhao, G.; McNerny, E.; Kohn, D. H.; Franceschi, R. T.; Holl, M. M. B.; Tecklenburg, M. M. J.; Ramamoorthy, A. Morris, M. D. Crystallinity and Compositional Changes in Carbonated Apatites: Evidence from ^{31}P Solid-State NMR, Raman, and AFM Analysis. *J. Solid. State. Chem.* **2013**, *206*, 192–198.

(13) Wang, Y.; Von Euw, S.; Fernandes, F. M.; Cassaignon, S.; Selmane, M.; Laurent, G.; Pehau-Arnaudet, G.; Coelho, C.; Bonhomme-Coury, L.; Giraud-Guille, M.-M.; Babonneau, F.; Azais, T.; Nassif, N. Water-Mediated Structuring of Bone Apatite. *Nat. Mater.* **2013**, *12*, 1144–1153.

Diffusive Attenuation Kernel

The pulse sequence used for the diffusion relaxation measurements is shown in figure S2. The attenuation of the magnetization due to the gradients was derived explicitly for the trapezoidal waveform, which was used in this work, using Mathematica. The spatial wavenumber is given by $q(t) = \gamma \int_0^t dt g(t)$, where $g(t)$ denotes the waveform of the gradient pulse. In the pulse sequence used in this work $g(t) = ct$ for the rising time interval ($\tau \rightarrow t_1$), $g(t) = G_m$ for the time interval ($t_1 \rightarrow t_2$) and $g(t) = -ct$ for the dropping time ($t_2 \rightarrow \delta$) and $c > 0$. To be clear, the rise and fall times of the trapezoidal gradient pulse are t_1 and $\xi \equiv (\delta - t_2)$, respectively. The attenuation factor is $-D \int_0^t dt q^2(t)$ and therefore the diffusive attenuation kernel is,

$$\begin{aligned}
\log \frac{M(g, t)}{M_0} = & \frac{\gamma^2}{30} \left[20G_m^2 (t_2 + \xi)^2 (9t_1 + 8t_2 + 8\xi + 6(\Delta + \tau)) + \right. \\
& c^2 \left(41t_1^5 + 15t_1^4 (3\xi + 2(\Delta + \tau) + 3t_2) - \right. \\
& 80\xi^2 t_1^3 - 10\xi^2 t_1^2 (7\xi + 6(\Delta + \tau) + 6t_2) + 45\xi^4 t_1 + \xi^4 (41\xi + 30(\Delta + \tau) + 45t_2) \left. \right) + \\
& 10cG_m \left(16t_1^3 (\xi + t_2) + 3t_1^2 (\xi + t_2) (5\xi + 4(\Delta + \tau) + 5t_2) - 18\xi^2 t_1 (\xi + t_2) - \right. \\
& \left. \left. \xi^2 (4\xi (4\xi + 3(\Delta + \tau)) + 15t_2^2 + 4t_2 (8\xi + 3(\Delta + \tau))) \right) \right]. \tag{1}
\end{aligned}$$

It should be noted that in eq. 1 the term proportional to Δ dominates for long times whereas the linear and non linear terms of t_1, t_2, ξ become important for short times.

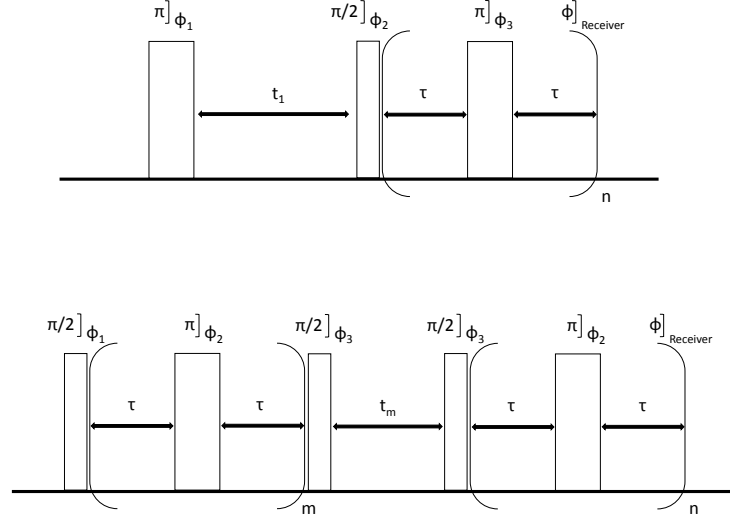


Figure S1: The radio frequency pulse sequences used for 2D $T_1 - T_2$ (top) and 2D $T_2 - T_2$ (bottom) experiments. The phase cycling used for 2D $T_1 - T_2$ experiments was, $\phi_1 = x, y, -x, -y$, $\phi_2 = x, x, -x, -x$, $\phi_3 = y, y, y, y$, and the receiver phase was $\phi_{\text{Receiver}} = x, x, -x, -x$. For 2D $T_2 - T_2$ experiments the phase cycling used was $\phi_1 = x, -x, x, -x$, $\phi_2 = y, -y, y, -y$, $\phi_3 = x, x, -x, -x$, and the receiver phase was $\phi_{\text{Receiver}} = x, -x, x, -x$

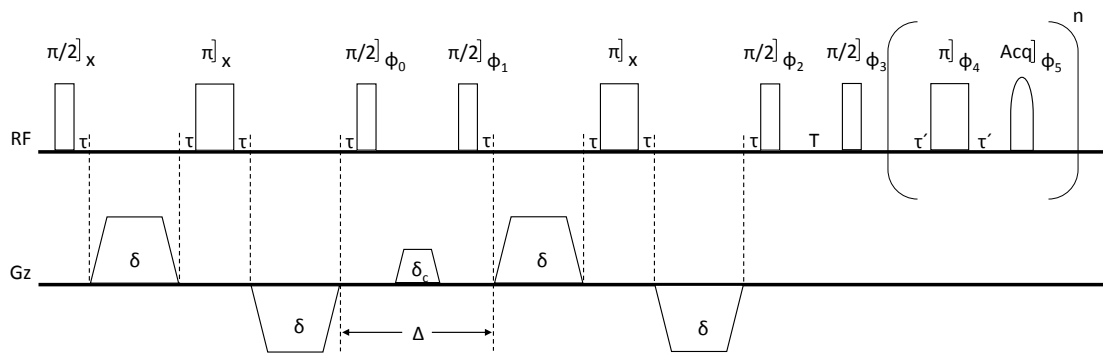


Figure S2: 2D diffusion- T_2 correlation pulse sequence. The first stage of the experiment makes use of a bipolar gradient stimulated echo pulse sequence introduced by Wu et al.¹ and the second part is a CPMG train. The π_x pulses refocus the background gradients. The use of bipolar gradient pulses compensate for the Eddy currents. In addition, shaped pulses were used to minimize ringdown effects which introduce imperfections in the gradient pulses. The phases $\phi_0, \phi_1, \phi_2, \phi_3$ and ϕ_5 of the RF pulses are given in¹ and an MLEV-16 phase alternating scheme was used for ϕ_4 . The kernel that describes the diffusive decay over the entire pulse sequence, given the trapezoidal pulses, is given by eq. 1.

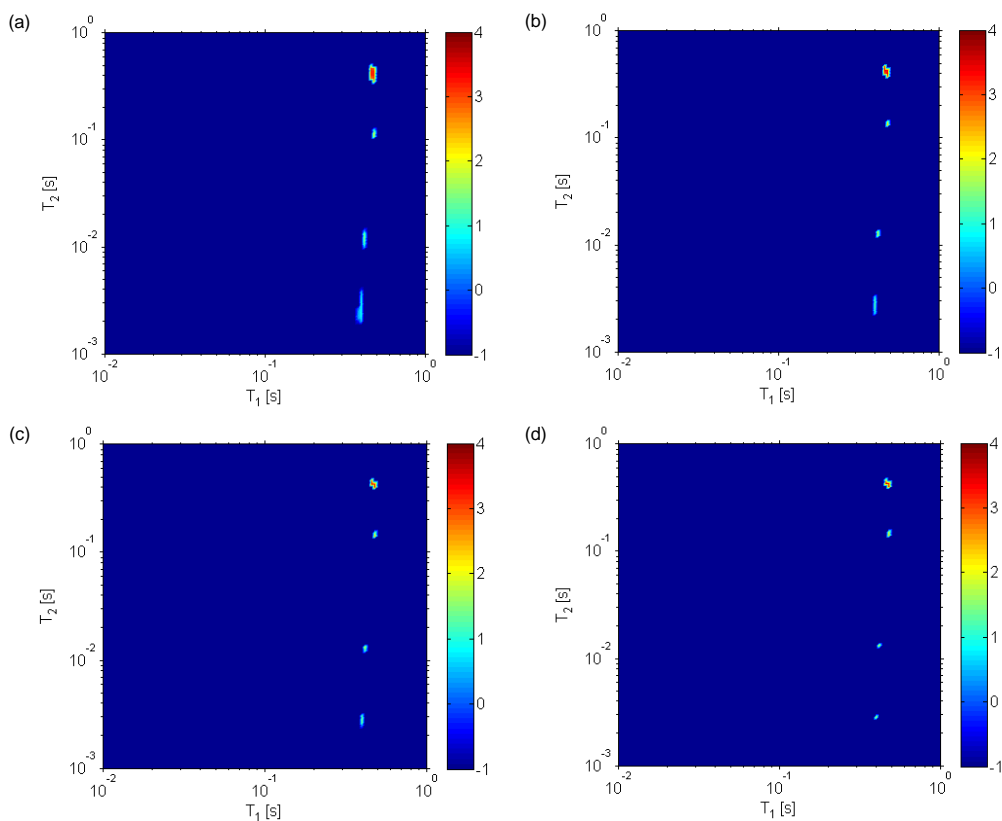


Figure S3: 2D ILT map of ^2H T_1 - T_2 experiments performed on untreated intact bone at 22°C , for different values of the regularization parameter α . In the figure the value of α was set to a) 0.5, b) 0.05, c) 0.005, and d) 0.0005. The relative signal intensities in the peaks A, B and C (see figure 1 in text) were observed to not vary significantly for the range of α shown (e.g. in a) the relative intensities of peaks A, B and C are 0.52, 0.30, and 0.018 and in d) the relative intensities are 0.61, 0.22, and 0.17 respectively.) Additionally, the centroid T_1 and T_2 values were also not observed to change significantly in the range of α shown. The BRD method gave a converged value of α in all our experiments that was approximately 10^{-4} . In this figure the color bar to the right, denoting signal intensity in arbitrary units, is on a logarithmic scale.

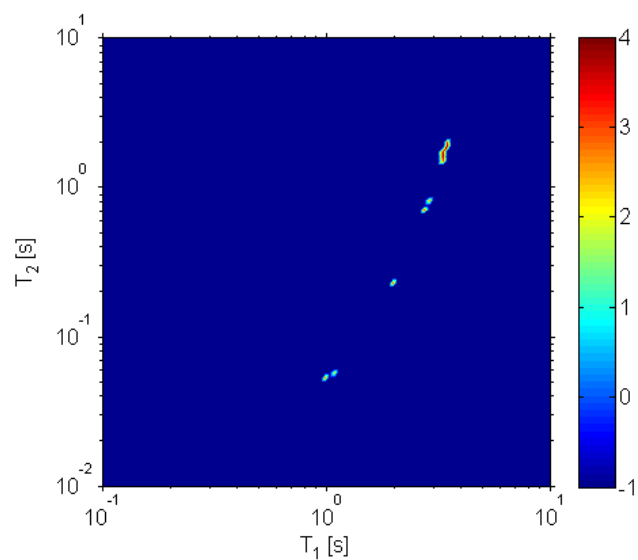


Figure S4: 2D ILT map of ^1H T_1 - T_2 experiments performed on untreated intact bone at 22°C . The experiment used a different values of τ and t_1 to measure the relaxation times T_1 and T_2 . Similar to the ^2H T_1 - T_2 experiments (figure 1a in the text), we observe 4 different reservoirs characterized by water experiencing different dynamical characteristics. In this figure the color bar to the right, denoting signal intensity in arbitrary units, is on a logarithmic scale.

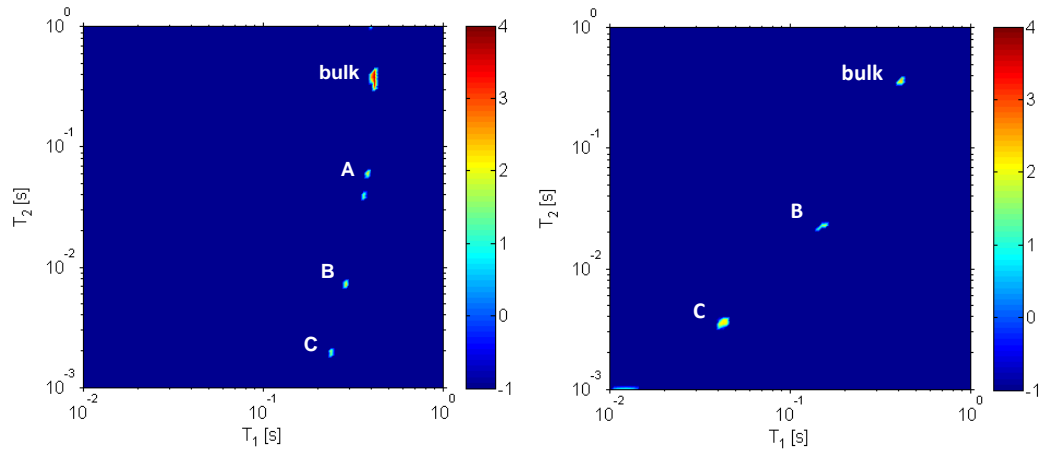


Figure S5: 2D ILT map of ^2H T_1 - T_2 experiments performed on untreated intact bone at 22°C. The left ILT map was obtained after immersing the bone sample in D_2O and the right ILT map was obtained after removal of D_2O from the NMR tube. These data reveal that peak A vanishes when bulk D_2O is removed providing evidence that this is peak arises from surface water on the bone samples. The values of the T_1 and T_2 relaxation times appear to change upon removal of the bulk water, as discussed in the text, and is likely evidence of exchange beyond what is probed in our T_2 - T_2 experiments (up to 10 ms). In this figure the color bar to the right, denoting signal intensity in arbitrary units, is on a logarithmic scale.

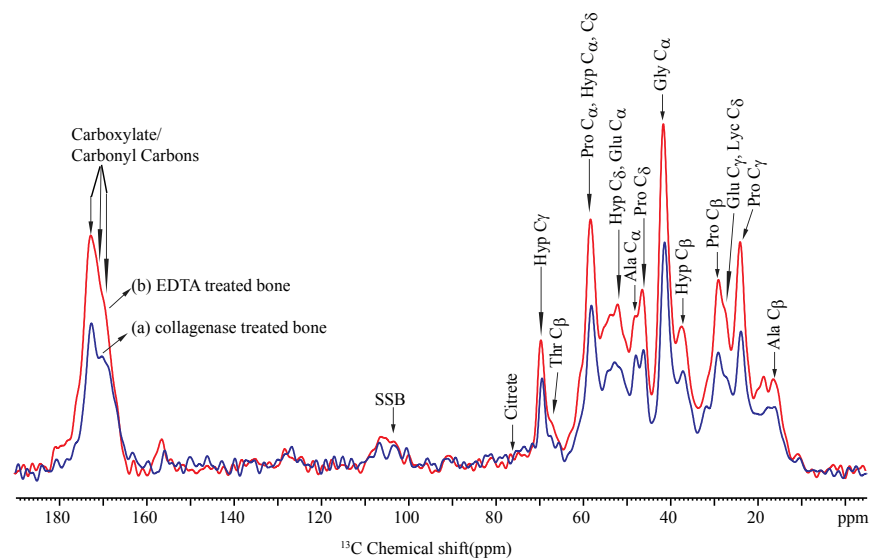


Figure S6: ^{13}C MAS NMR spectra of a) collagenase treated and b) EDTA treated bone sample recorded at 10 kHz magic angle spinning speed.

References

- (1) Wu, D.; Chen, A.; Johnson, C. S. An Improved Diffusion-Ordered Spectroscopy Experiment Incorporating Bipolar-Gradient Pulses. *J. Magn. Reson. Series A* **1995**, *115*, 260–264.